Scientific Open Access Journals
SOAJ

Journal of Toxicology and Pharmacology

Research Article | Open Access

In Vitro Cytotoxicity of Water Soluble Silver (Ag) Nanoparticles on Hacat and A549 Cell Lines

Mary Garvey[1,2,3]*, Sibu C. Padmanabhan[4,5]*, Suresh C. Pillai[3,6], Malco Cruz-Romero[7], Joseph P. Kerry[7] and Michael A. Morris[5]

[1]Department of Life Sciences, Institute of Technology Sligo, Sligo, Ireland

[2]Cellular Health and Toxicology Research Group, Institute of Technology Sligo, Sligo, Ireland

[3]Centre for Precision Engineering, Materials and Manufacturing Research (PEM), Institute of Technology, Sligo, Ireland

[4]Department of Chemistry, University College Cork, Cork, Ireland

[5]Advanced Materials and BioEngineering Research (AMBER), Trinity College Dublin, College Green, Dublin, Ireland

[6]Nanotechnology Research Group, Department of Environmental Science, Institute of Technology Sligo, Ireland

[7]Food Packaging Group, School of Food & Nutritional Sciences, University College Cork, Cork, Ireland

***Corresponding author: Mary Garvey & Sibu C. Padmanabhan,** Email: garvey.mary@itsligo.ie; sibucp@yahoo.com / sc.padmanabhan@ucc.ie

Received: 27 October 2017; **Accepted:** 21 December 2017; **Published:** 26 December 2017

Abstract

The wide range of applications of silver nanoparticles (AgNPs) in commercial products, including food packaging, has encouraged researchers to come up with novel preparation methods for the production of these robust materials. The methods resulting in the formation of NPs for such commercial applications clearly demand a good accounting of their toxicity aspects to humans as well as the environment. We herein present a chemical preparation method for the production of size- and shape-defined AgNPs and investigate the impact of these nanoparticles on HaCat and A549 cell lines. Findings show that lung cells (A549) are more sensitive than skin cells (HaCat) to Ag induced toxicity, evident by the significantly ($p<0.05$) reduced LC50 for all NPs under study. The current investigation showed that the extent of surface capping agent (citrate) and size influenced the cell toxicity, where a lesser surface coverage (zeta potential, ζ, -27.7 mV) and smaller size (~17 nm) enhanced the toxicity compared to comparatively bigger particles (~39 nm) with higher surface coverage (ζ, -47.3 mV). The size- and shape-defined particles such as triangles which have proven useful for many applications, due to their high energy/high field edges, were found to be less toxic against biological cell lines and therefore may have potential to be used in food packaging applications as reservoirs of silver ions. A striking difference in cell line toxicity within such a small size window clearly demonstrates the vital roles played by the smaller size, difference in shape and lesser surface coverage in defining a higher passive cell membrane diffusion followed by silver dissolution inside cell cytoplasm increasing cytotoxicity.

Keywords: Silver nanoparticles; Cytotoxicity; Lung cell; Skin cells

Introduction

In recent years, metal nanoparticles (NPs) have attracted much attention in many areas such as microbiology, nano-biotechnology and the manufacture of commercial products. Metal NPs exhibit distinctive and significantly altered physical and chemical properties, in comparison to their macro-scaled equivalents [1]. The use of NPs has become rudimentary in the manufacture of numerous consumer items such as personal care products (PCPs), household materials, textiles and medical products [2]. Due to their antimicrobial nature and vast consumer applications, AgNPs have become the most widely used commercially available nanoparticles [3]. Recently, research on applying AgNPs for food packaging applications has intensified due to its very effective and wide-spectrum antimicrobial properties [4-9].

With the use of AgNPs as antimicrobials in catheters and wound dressings [10] they have the ability to enter human tissues and cells where they may elicit an undesired effect *in vivo*. The presence of AgNPs in personal care products allows for a transdermal route of entry. The presence of AgNPs in food packaging can enter the human tissues and cells and may evoke undesired effects if they are migrated to the food in uncontrolled quantities [8]. Their recent extended use has arisen serious concern relating to the impact of these NPs on human health and environmental niches following prolonged exposure [1]. Deliberate and accidental exposure to NPs, such as AgNPs, primarily occurs by dermal contact, inhalation and ingestion. However, the lung is regarded as the least protected organ and the main portal entry of NPs, where they can subsequently enter the alveoli, the deepest part of the respiratory tract [11]. Studies assessing the distribution of AgNPs following inhalation and intra-tracheal instillation in animal models found AgNPs present in the lungs, blood circulation, liver, kidneys, spleen, heart and brain [2]. Studies by Takenaka et al. showed that NPs distribute around the body via the circulatory system and found AgNPs deposited in the lungs following inhalation in rats [12]. Studies have shown that mammalian cells can accumulate NPs via pinocytosis, endocytosis, clathrin-dependent endocytosis and phagocytosis [13]. These routes of uptake, intracellular localisation and exocytosis depend on the fundamental characteristics of nanoparticles i.e. size, surface characteristics, ζ and its resistance to accumulation [13]. Additionally, the uptake of NPs can vary depending on cell types where they induce cytotoxicity by a number of means. Mukherjee et al. carried out cytotoxicity studies of commercial silver nanopowder [1]. They concluded that the Reactive Oxygen Species (ROS) production of silver nanomaterials during the entry of the cell wall as one of the major steps which lead to cell death. The production of ROS by silver nanoparticles is largely depended on the synthesis conditions, surface capping agents and morphology [14-20].

Controlling the shape and/or size of AgNPs is reported as an important methodology to employ these materials for various

applications in the fields of antimicrobial agents [7,21], catalytic materials [22], biomedical applications [23] and Surface Enhanced Raman Spectroscopy (SERS) [24]. In particular, in food packaging applications, the effect of their size, shape and capping agents can play a crucial role in their dissolution and migration into the food product. Therefore it is essential to assess the toxicity effects of size- and shape-defined NPs *in vitro* and *in vivo* on cell lines to establish the biocompatibility or toxicity of these NPs for use in food packaging materials. The current work reports the effects of size, morphology and the extent of citrate surface coverages of AgNPs, prepared by a controlled seed-catalysed growth method, on their cytotoxicity against HaCat and A549 cell lines. In fact, there have been a number of study reports discussing the size-dependent toxicity of silver NPs [25,26]. However, the findings are not yet conclusive as each set of particles present its own complexity in terms of their varying properties that can be mutually connected and hence difficult to pin point and correlate to the cytotoxicity [27], which warrants more studies especially with respect to new synthesis procedures and particles prepared. In light of this, a small size window ranging from ~17 nm (AgG7) to ~39 nm (AgG2) where the particles show two types of prominent shape features such as disc-like (AgG7 and AgG4) and triangular (AgG2) are selected to understand their usefulness/issues for food packaging applications. This study, therefore, would contribute greatly to the knowledge-base on antimicrobial silver based innovative technology solutions being developed for food packaging applications.

Experimental section

Synthesis of NPs

All chemicals used for NPs synthesis were sourced from Sigma-Aldrich Ireland Ltd, Ireland. In a typical experiment, silver seeds are produced by combining aqueous trisodium citrate (5 mL, 25 mM), aqueous poly(sodium styrenesulphonate) (PSSS; 2.5 mL, 500mg L^{-1}; Aldrich 1,000 kDa) and aqueous $NaBH_4$ (3 mL, 10 mM, freshly prepared) in 45 mL of Millipore water (MPW) followed by addition of aqueous $AgNO_3$ (5 mL, 5 mM) at a rate of 2 mL min^{-1} while stirring continuously. The nanoparticles are then grown by combining 85 mL MPW, aqueous ascorbic acid (0.8 mL, 10 mM) and various quantities of seed solution (seed concentrations such as 2, 4 and 7 mL, named as AgG2, AgG4 and AgG7 respectively, were selected for this study), followed by addition of aqueous $AgNO_3$ (10 mL, 2.5 mM) at a rate of 0.5 mL min^{-1}. At the end of addition, aqueous trisodium citrate (5 mL, 25 mM) is added to stabilize the particles, stirred for 5 mins and kept in the dark until used. The rationale for selecting samples AgG2, AgG4 and AgG7 in this study is their difference in characteristics (such as particle size, morphology and surface coverage) in a tight size window i.e. between ~17 nm and ~39 nm. Test concentrations of 1, 2, 10 and 20 ppm of the above NPs were tested using a number of biocompatibility assays with varying endpoints.

Characterization

UV-Vis absorption spectra were obtained from diluted samples using a Thermoscientific evolution 60 spectrophotometer. Transmission electron microscopy (TEM) images were taken using a JEOL JEM-2100 microscope at 200kV. ζ and hydrodynamic particle size distribution (PSD) of the NP sols were measured using a Malvern NanoZS Zetasiser. The average of three consecutive measurements was taken as the final ZP and PSD readings (ESI). pH measurements (EL 20 pH meter, Mettler Toledo, Switzerland) were taken for test NPs both in the absence and presence of cell culture media to determine if any pH changes occurred which may negatively impact the cells.

Cell culture

Monolayers of the human keratinocytes cell line HaCat (ATCC American Type Culture Collection, Rockville, Md.) and human lung carcinoma cell line A549 (ATCC CRM-CCL-185) were grown with regular sub-culturing in DMEM growth media with L-glutamine and supplemented antibiotics (penicillin G, 100,000 U/L, streptomycin, 500mg L^{-1} and amphotericin B, 500mg L^{-1}), sodium bicarbonate, 2 g L^{-1}, and 10 % foetal calf serum adjusted to pH 7.4. Both cell lines were cultured and maintained in T75 cm^2 cell culture flasks (Sarstedt, Germany) in a humidified incubator at 37 °C in an atmosphere containing 5 % (vol/vol) CO_2 for circa. 24 h until 80 to 90 % confluent monolayers had formed. Once confluent, cells were trypsinised with trypsin 0.25 % to remove the cell monolayer from the flask and seeded into 96 well plates for 24 h at 37°C at a seeding density of 1 x 10^5 cells/well for cytotoxicity studies. All cell culture media and its contents were sourced from Sigma-Aldrich Ireland Ltd, Ireland.

MTT Assay: The method determines the activity of the mitochondria of viable cells by measuring the ability of mitochondrial succinate dehydrogenase to convert the tetrazolium salt MTT to a dark blue/purple formazan product. The amount of formazan produced can be taken as a direct measure of cell viability. A 5mg mL^{-1} MTT (Sigma-Aldrich Ireland Ltd, Ireland) stock solution was prepared by adding 50mg MTT to 10 mL sterile phosphate buffered saline (PBS) (Sigma-Aldrich Ireland Ltd, Ireland) in a sterile universal, the solution was stored in the dark at 4 °C and pre-heated by incubating at 37°C for 1 hr prior to use. The MTT solution was filter sterilised using a 0.2μm pore sized syringe filter to remove any crystal which had formed. Dimethyl sulfoxide (DMSO) (Sigma-Aldrich Ireland Ltd, Ireland) was used to extract and solubilise the formazan precipitate. Cytotoxic effects on both cell types was determined using 96 well microplates (Sarstedt, Germany) seeded with 1 x 10^5 cells in 200μL of complete culture medium. The plates were then incubated for 12-24 hr at 37°C until the desired percentage of confluency (80 %) was observed. Cells were exposed to nanoparticle test samples by adding 20μL of sample with 180μL of cell culture media to the cells in triplicate for 24 hrs. Subsequently after 24 hr incubation the medium containing test chemicals was discarded and the wells were washed twice with pre-heated PBS. After the washing step 180μL of fresh media and 20μL of MTT solution was added to each well to obtain a final MTT concentration of 0.5mg mL^{-1}. Following an additional 4 hr incubation period at 37°C, the MTT containing medium was carefully aspirated off and resulting blue formazan crystals were

solubilised by the addition of 100µL of DMSO to each well. To support solubilisation the plates were shaken gently and the optical densities of each well recorded using a multiwell plate reader (Fluostar Otima, BMG Labtech, Ortenberg, Germany) at a test wavelength of 540 nm and a reference wavelength of 690 nm. Results are presented as percentage of untreated controls against test chemical concentrations.

LDH Assay: The LDH Cytotoxicity Assay Kit (Thermo Scientific™, Dublin, Ireland) is a colorimetric assay kit which quantitatively measures lactate dehydrogenase (LDH) released into the media of damaged cells as an indicator of cell damage or cytotoxicity. Cells were seeded in a 96 well plate at 1 x 10^5 cells/well and incubated at 37°C to allow for cell adherence and monolayer formation. Cells were then exposed to AgNPs in cell culture media for 24 hrs as per assay conditions. The LDH assay was then performed as described in the kit guidelines (LDH procedure for "Chemical Compound-Mediated Cytotoxicity Testing"). Subsequently, the plates were read using a multiwall plate reader at 490 nm and 680 nm as per the kit instructions.

Cell count assay: Cells which had reached 90 % confluency in a T25 cell culture flask (Sarstedt, Germany) were trypsinised and re-seeded in to a 6 well plate (Sarstedt, Germany) at a concentration of 1 x 10^5 cells/mL in 2 mL final volumes. Plates were incubated at 37 °C for 12 hrs with 5 % CO_2 to allow for monolayer attachment. Following the incubation period the cell media was removed and cell monolayers were washed with sterile pre-heated (37°C) PBS. Fresh media was added to the untreated control wells (2 mL) and media containing AgNPs was added in replicate to treated monolayers, 200µL nanoparticles with 1800µL media. Cells were again incubated at 37 °C for 24 hrs with 5 % CO_2 to allow for nanoparticle effect on treated cells. After which, the media was removed from all cell monolayers which were subsequently washed with sterile PBS and trypsinised for 5 mins to remove the attached cells. Cells were removed from the individual wells and centrifuged at 4000 rpm for 5 mins followed by suspension in sterile PBS containing trypan blue (Sigma-Aldrich Ireland Ltd, Ireland). 10µL volumes were transferred to a haemocytometer to perform a viable cell count of treated and untreated cells.

Statistics

All experiments were conducted in three replicates with at least 4 internal replicates per plate. Cytotoxicity induced from AgNPs was measured as a percentage of the untreated control using the formula % cytotoxicity = $(N_t/N_0)*100$ where No is untreated control and Nt is treated sample. All LD_{50} values were calculated using the average cytotoxicity data of the three independent experimental replicates (+/- standard deviation). Standard T tests were used to determine the sensitivity of each cell line to AgNPs exposure ($p \leq 0.05$), and to compare the toxicity of the varying nanoparticle types.

Results

Characterisation of AgG nanoparticles

The AgNPs were prepared here by a slow, controlled growth process by using ascorbic acid as reductant and stabilized them subsequently with trisodium citrate molecules. Figure 1a presents the UV-Vis extinction (absorption and scattering) spectra of aqueous AgNP solutions prepared by the described chemical reduction method. The seed solution, AgS, shows a

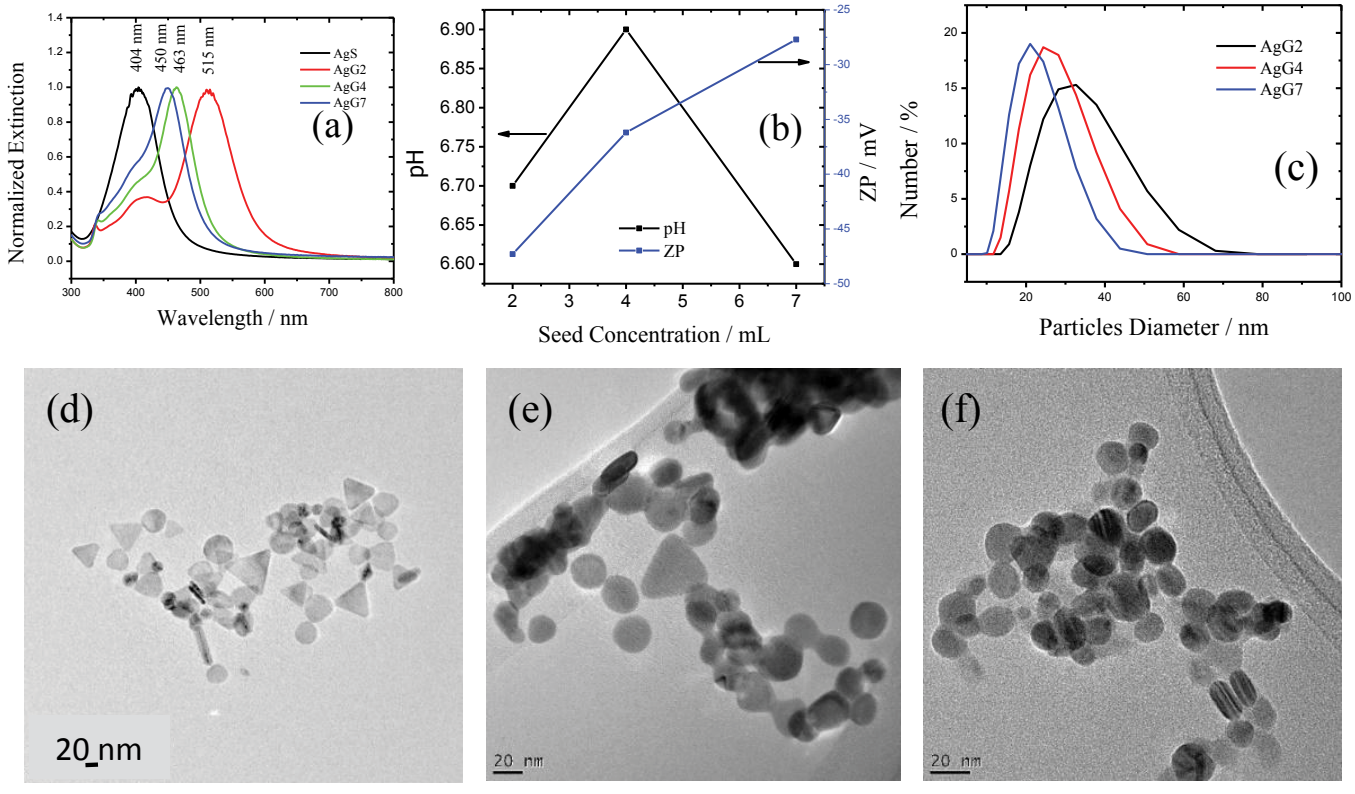

Figure 1: (a) UV-Vis extinction spectra, (b) plots of ZP and pH *vs* seed concentration, (c) DLS particle size distribution and TEM micrographs of AgNPs prepared from seed (AgS) concentrations of (d) 2 mL (AgG2), (e) 4 mL (AgG4) and (f) 7 mL (AgG7).

λ_{max} of 404 nm. The major peaks observed (515, 463 and 450 nm) for AgG2, AgG4 and AgG7 NPs are as a result of the surface plasmon resonance (SPR) absorption (in-plane dipole) and scattering of AgNPs of particular size and shape [18,19]. The shoulder-like peaks observed in all three spectra at ~400 - 417 nm is due to the in-plane quadrupole resonance absorption. The peaks observed in the region 337 - 342 nm is ascribed to the out-of-plane quadrupole resonance. The different λ_{max} observed for different samples implies its different size and shape. TEM was taken to understand and correlate the influence of NP size and shape on the optical properties. Figures 1d - 1f present the TEM micrographs of samples AgG2, AgG4 and AgG7 respectively. Particle sizes measured from these TEM images (and those not presented here) show that 2 mL seeded-growth (AgG2) produced NPs in the size range of 39 ± 28 nm. 4 mL seeds (AgG4) produced 28 ± 16 nm, and 7 mL seeds (AgG7) yielded NPs of 17 ± 4 nm. It can be seen that the bigger particles produced from 2 mL seeds contain more number of triangular particles, the occurrence of which diminishes on increasing the seed concentration to 4 mL; and 7 mL seeds produce only very few triangular particles. The shift of in-plane dipole of NPs observed in the UV-Vis spectra is consistent with this obvious difference in size and shape of formed NPs [28]. The larger edge length of triangles obtained for AgG2 sample as compared to the smaller sizes/edge lengths for AgG4 and AgG7 samples is also reflected in their in-plane quadrupole resonance band where when AgG2 shows a well-developed band at 417 nm the prominence of it can be seen fading out for the other two samples. It can also be noted that almost all of the particles have grown into disc-like particles (triangles and/or discs), as also evidenced from the in-plane resonance absorption bands, with very few exceptions where some have acquired twinned sphere-like structure with multiple edges. The ζ values obtained are -47.3, -36.2 and -27.7 mV respectively for samples AgG2, AgG4 and AgG7 (Figure 1b). The PSDs (figure 1c) and polydispersity indices (PdIs) obtained from dynamic light scattering (DLS) studies are also consistent with the TEM result which are 22.13 nm and 0.364; 22.04 nm and 0.203; and 19.81 nm and 0.119 respectively for AgG2, AgG4 and AgG7. It is to be noted here that though the PSDs show only slight difference, the difference in PdI accounts for the varying particle sizes obtained from TEM. All AgNPs were determined to be in a range of pH 6.5 to 7 and this did not change significantly when NPs were diluted in cell culture media before application onto the cell monolayers.

Cytotoxicity studies

There was a significant cytotoxicity of both lung and skin cells as detected via the MTT assay. Figure 2 shows that all concentrations tested produced high levels of cytotoxicity of lung cells e.g. with a concentration of 20 ppm there was greater than 90 % toxicity for all NPs tested. A significant loss of viability was seen for test concentrations of 1, 2 and 10 ppm, showing a dose response relationship for treated lung cells. AgG4 and AgG7 proved more toxic to lung cells than AgG2, where the LC_{50} was found to be 0.86, 0.15 and 0.14 ppm for AgG2, AgG4 and AgG7 respectively. Interestingly, size analysis shows that AgG2 (39 nm) is larger in size than AgG4 (28 nm) and AgG7 (17 nm). Findings show that for treated skin cells (HaCat) a change in the pattern of toxicity occurred, whereby with an increase in NP concentration a decrease in toxicity was observed (Figure 2). The LC_{50} for AgG2, AgG4 and AgG7 on treated HaCat cells was found to be 16, 17.5 and 18 ppm respectively. Therefore, the level of toxicity did not follow a typical dose response relationship, evident from the unexpected pattern of viability shown. Additionally, the HaCat skin cell line proved less sensitive to AgNPs insult when treated *in vitro* than

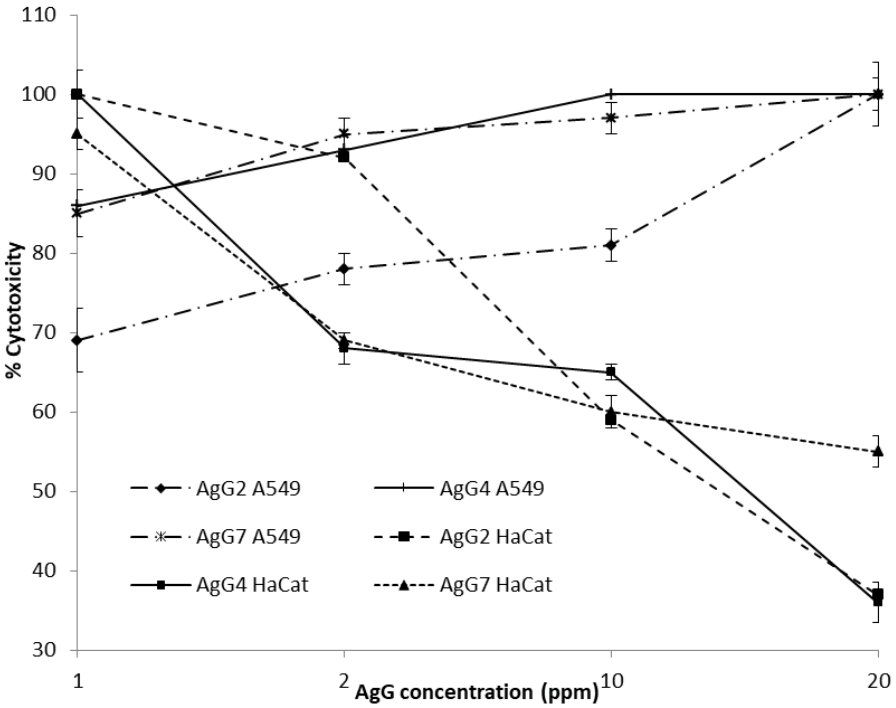

Figure 2: Cytotoxicity of lung cells (A549) and skin cells (HaCat) following exposure to various silver nanoparticles for 24 hours (+/-S.D) at varying concentrations (ppm) as determined by the MTT assay (+/-S.D).

the A549 lung cell line. A concentration of 20 ppm resulted in 37, 36 and 55 % cell death for AgG2, AgG4 and AgG7 respectively.

Findings show (Figure 3) that NP induced toxicity did not follow a typical dose response pattern when assessed via the LDH assay. There was no pattern evident indicating that an increase or decrease in NP concentration resulted in increased toxicity as with the MTT assay. However, for both cell types a concentration of 1 ppm of all test NPs provided the highest level of cell death with up to 100 % cytotoxicity of the HaCat cell line. For both cell types under study no cell death was detected for 20 ppm NP solutions. Again the A549 cell line proved more sensitive than the HaCat when exposed to AgNPs at a concentration of 2 and 10 ppm. Due to the erratic nature of the data it was not possible to determine an LC_{50} for either cell line.

Figure 4 depicting the results of the cell count assay show similar levels of toxicity to the MTT assay for both cells lines treated with 20 ppm NPs e.g. a ca. 90 % loss of A549 cell viability occurred following 24 hr exposure to each test NP. Indeed, comparable values were obtained for each concentration tested (data no shown). There was no significant difference ($p<0.05$) in cytotoxicity observed for each NPs tested on lung cells, with all 3 samples providing greater than 85 % cytotoxicity. The LC_{50}

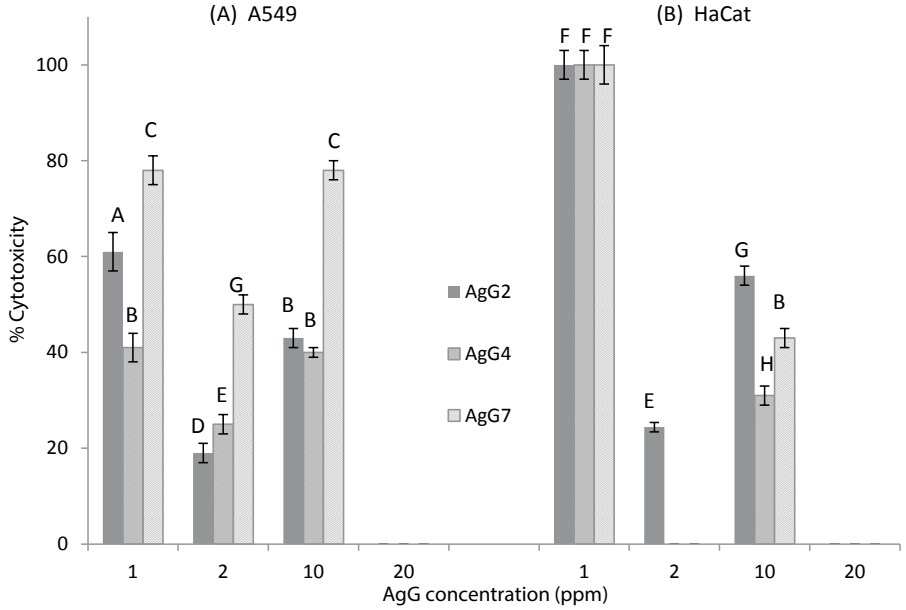

Figure 3: Cytotoxicity of (A) lung cells (A549) and (B) skin cells (HaCat) following exposure to various silver nanoparticles for 24 hours (+/-S.D) at varying concentrations (ppm) as determined by the LDH assay. A, B, C, D, E, F and G denotes significant difference ($p \leq 0.05$).

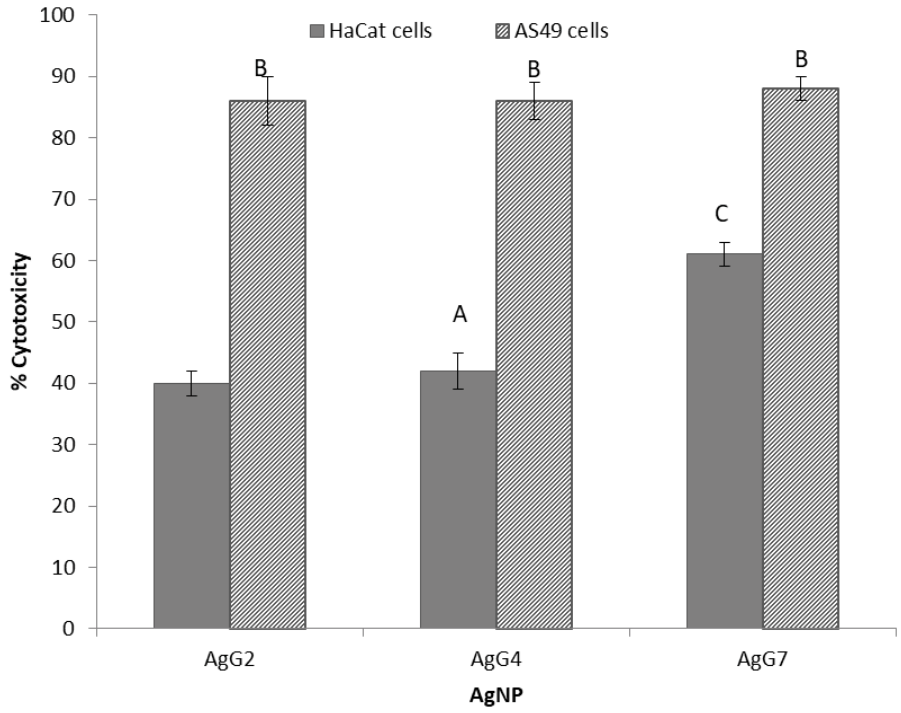

Figure 4: Cytotoxicity of lung cells (A549) and skin cells (HaCat) following exposure to various silver nanoparticles for 24 hours (+/-S.D) at 20 ppm as determined by viable cell count assay. A, B, and C denotes significant difference at $p \leq 0.05$.

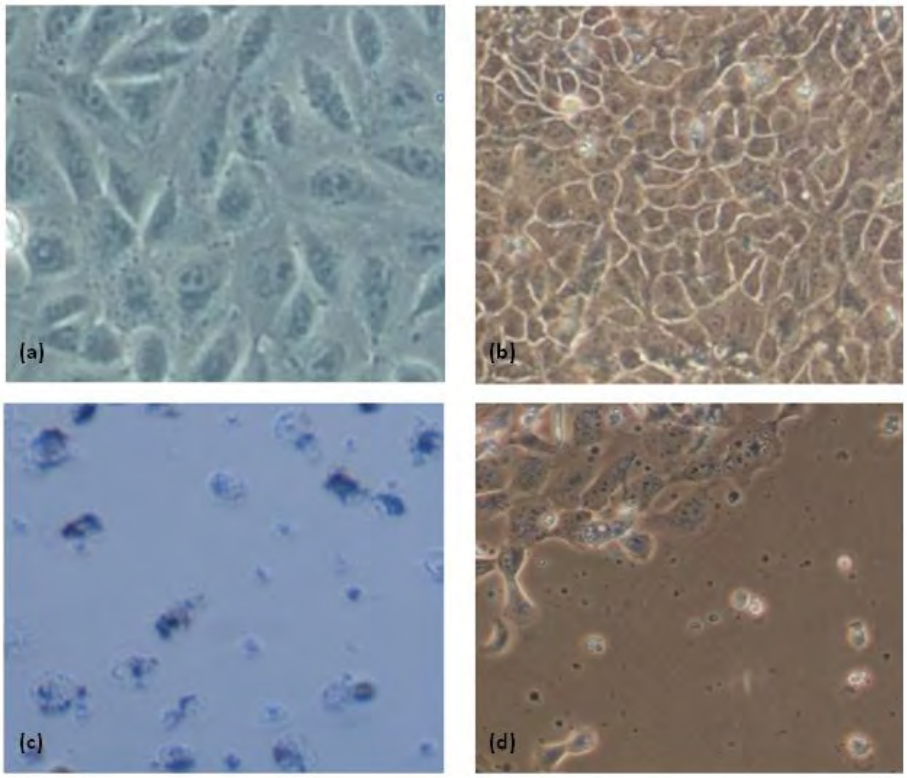

Figure 5: Images of (a) untreated control A549 cells and (b) untreated HaCat cells, (c) 24 hour treated A549 and (d) HaCat cells with 20 ppm AgG7.

for AgG2, AgG4 and AgG7 was determined to be 0.80, 0.20 and 0.15 ppm respectively. Additionally, the HaCat skin cell line proved less sensitive to NP exposure with approximately 40, 42 and 60 % cytotoxicity observed for AgG2, AgG4 and AgG7 respectively, comparable to the MTT assay. The LC_{50} for AgG2, AgG4 and AgG7 on treated HaCat cells was found to be 3.0, 3.21 and 3.10 ppm respectively. Microscopic observation of untreated (Figure 5a and b) and treated cells (Figure 5c and d) show that extensive damage to both cell monolayers occurred following incubation with AgG7 NPs. Figure 5 shows a significant loss of monolayer integrity following 24 hr incubation with 20 ppm AgG7 which occurred for all test solutions and concentrations (data not shown) to varying degrees. The extensive cell damage and monolayer destruction depicted in these images following exposure to 20 ppm AgG7 highlights the contradictory findings of the LDH assay and confirms the findings of the MTT assay.

Discussion

Due to the increasing applications of nanoparticles in everyday life it is essential to determine the toxicity levels (observed effects or lethal concentration) for these robust materials. Studies described herein are intended to determine cell viability in the presence of silver nanoparticles prepared for food packaging applications. The cell viability was assessed by determining mitochondrial function (MTT assay) and membrane leakage (LDH assay) in human lung and skin cell lines. Findings show that a dose-dependent increase in cell death occurred for each NP under study as assessed by the MTT assay. Predictably, with an increase in NP concentration an increase in toxicity was observed for the lung cell line. NP AgG7 proved the most lethal to the A549s with an LC_{50} of 0.14 ppm. Interestingly, NP AgG7 was also the smallest of the nanoparticles tested with an average size of 17 nm as determined by TEM image analysis and had the smallest ζ at -27.7 mV. AgG4 had a similar (not significantly different at $p \leq 0.05$) LC_{50} of 0.15 ppm on lung cells with an average size of 28 nm and ζ of -36.2 mV. The largest NP AgG2 (39 nm, ZP -47.3) had the greatest LC_{50} of 0.83 ppm. Research has shown that smaller NPs can more readily cross the cell membrane entering the cytosol of the cell than larger NPs of the same metal [19]. The MTT assay is based on mitochondrial function; therefore, NPs must enter the cytosol to have a measureable effect, deleterious or otherwise. The role of mitochondria in cell death pathways has been well established, whereby a loss of mitochondrial function leads to stimulation of apoptosis and a loss of cellular respiration [29]. It was previously reported that smaller NPs display greater toxic effects than larger NPs due to their high surface area increasing the interaction of NPs with cellular biomolecules [26,30]. Research has indicated that cell uptake of NPs of less than 50 nm [31] can occur by endocytosis, which includes the AgNPs described in this study. Additionally, the formation of O_2^- by the citrate-stabilized AgNPs can be considered as one factor that induces cytotoxicity to all AgNPs studied here [11,16]. Further, the surface coverage of three samples studied clearly varies as evidenced by the ZP results, where AgG7 has the lowest surface coverage. The lower surface potential could also facilitate an easier dissolution and release of silver as Ag^+ into the cell media thus facilitating cell attack and subsequent cell death [14,18,32].

A loss of mitochondrial activity was seen in HaCaT cells following 24 hr exposure to AgNPs as measured by the MTT assay, at all concentrations tested. However, the LC_{50} values for

all AgG samples with the MTT assay was significantly higher for the HaCat cells than the A549 cell line. This increased resistance to Ag toxicity is in keeping with the findings of Zanette et al. where AgNPs at a concentration of 3 ppm were shown to have an inhibitory effect on HaCat cell growth as opposed to resulting in cell death (cytotoxicity). Indeed, the findings described concluded that in HaCaT cells AgNPs do not elicit cytotoxic, necrotic events but have effect on the ability of cells to proliferate over a 24 hr period [33]. Additionally, it is worth noting that skin cells by nature have a reduced number of mitochondria compared to lung cells due to the demand of their pulmonary activity. Therefore, assessing cytotoxicity as determined by mitochondrial function may imply an increased sensitivity of cells high in mitochondrial content. Findings showed that with an increase in AgG concentration a reduction in cytotoxicity occurred for the HaCat cells. One possible suggestion for this behaviour may be due to NP aggregation; however this does not explain the typical dose response seen in lung cells following exposure. Research has also shown that ultralow concentrations of AgNPs favour complete solubility as Ag^{+} and to its possible complexes [19].

Additionally, all NPs tested have an overall net negative ζ. As reported by Gemgam et al. ζ greater than 30 mV or less than -30 mV suggests the presence of stable nanoparticles [34]. The negative charge on all synthesised AgNPs implies that aggregation is unlikely to occur due to the strong repulsive forces among the silver NPs. Therefore, the NP's under investigation are deemed to be relatively stable. Recent reports have shown that the measurement of the cytotoxic potential of silver nanoparticles in mammalian cells results in large variability, with concentrations causing 50 % viability reductions varying amongst cell types.

Typically, *in vitro* cytotoxicity assays are chosen to assess NP toxicity with endpoints based on spectrophotometric readings at suitable wavelengths due to their rapid and reproducible nature. Furthermore, many of these assays are reliant on complicated biochemical reactions which lead to a change in absorbance or fluorescence, consequently providing information on physiological or biochemical endpoints [35]. However, the distinctive physicochemical properties and increased reactivity of NPs means that there is a possibility that these materials may interfere with assays based on such endpoints. Studies by Oh et al. reported that their silver NPs had an effect on ROS production which inactivates LDH and NPs adhered to essential proteins resulting in inaccurate data from this assay [36]. The LDH assay is based on the release of the cytosolic enzyme lactate dehydrogenase (LDH) into the culture medium. The binding of NPs to biomolecules such as proteins present in cell media is a previously identified issue; additionally NP size is believed to play an important role in this interaction [30]. The authors believe that such interference occurred with the LDH assay leading to erratic data. A notable possibility is the interference of AgNP's absorption (colour) with the absorbance being recorded in LDH assays. Especially in LDH assay, all AgNP's absorptions interfere with the 490 nm reading thereby possibly causing the erratic data. The interference would be lesser when lower concentrations (3 ppm and below as reported here) of NPs are used as the NP absorbance will be overpowered by the assay sample absorbance. However the corroboration between MTT assay and cell count results confirm that the AgNPs studied here are all cytotoxic to the studied HaCat and A549 cell lines, where the smallest AgNP studied (AgG7) shows the maximum cytotoxicity. This could be attributed to the combined effects of smallest size and lower surface coverage, ζ, facilitating passive cell membrane diffusion and easy dissolution/complexation inside the cell cytoplasm. Alternatively, the highest surface energy (surface area) for AgG7 may facilitate a greater NP-cell interaction and/or the creation of detrimental ROS, especially super oxides (O_2^{-}). In this case, however, the passive diffusion by AgG7 and following silver-dissolution and complexation with amino and sulfidic molecules in the cell cytoplasm are believed as the mechanism of cytotoxicity [37]. The slightly larger size for AgG4 and AgG2 samples and especially their more triangular shape features with a larger surface coverage, ζ, hence protection, are attributed here as the reason for a lesser passive cell membrane diffusion causing less cytotoxicity.

Conclusions

Findings show that chemically produced water soluble citrate capped AgNPs studied here are toxic to the A549 and HaCat cell lines and the toxicity is attributed to their smaller size and extent of surface coverage allowing them easier passive diffusion and dissolution in the media under study. The results also proves that bigger particles are less toxic and therefore promising to be used in food packaging applications. In detail, however, the HaCat cell line proved less sensitive to Ag toxicity than the lung cells as seen by the greatly increased LC_{50} values. Further, there are notable differences between the results of LDH and MTT assays for all AgNPs tested and conclude that the LDH assays failed to accurately detect cytotoxicity. The interference of AgNP absorption is attributed to this discrepancy in LDH assay. The aim of this study was to look at the effect of size-, shape- and surface citrate-coverage of silver nanoparticles prepared within a narrow size window to critically understand their effect as a food packaging active component. The results show that the bigger particles studied (~39 nm) are less toxic to the cell lines tested. This indicate that the use of these particles as preformed NPs can be applied in food packaging materials as they could act as reservoirs of silver ions releasing them in a controlled manner thus reducing the issues of uncontrolled migration of silver into the food in question.

Conflict of Interest

The authors declare that there is no conflict of interest.

Acknowledgements

The authors acknowledge Enterprise Ireland Commercialisation Fund (CF/2014/4370), Science Foundation Ireland through the AMBER Research Centre Grant (12/RC/2278) and National Development, through the Food Institutional Research Measure (FIRM) administered by the Department of Agriculture, Food and the Marine (Project no. 11/F/038) for their financial support.

References

1. Mukherjee SG, O'Claonadh N, Casey A, Chambers G. Comparative in vitro cytotoxicity study of silver nanoparticle on two mammalian cell lines. Toxicol In Vitro. 2012; 26:238-51.
2. Chairuangkitti P, Lawanprasert S, Roytrakul S, Aueviriyavit S, Phummiratch D, Kulthong K, et al. Silver nanoparticles induce toxicity in A549 cells via ROS-dependent and ROS-independent pathways. Toxicol In Vitro. 2013; 27:330-8.
3. de Lima R, Seabra AB, Duran N. Silver nanoparticles: a brief review of cytotoxicity and genotoxicity of chemically and biogenically synthesized nanoparticles. J Appl Toxicol. 2012; 32:867-79.
4. Fedotova AV, Snezhko AG, Sdobnikova OA, Samoilova LG, Smurova TA, Revina AA, et al. Packaging materials manufactured from natural polymers modified with silver nanoparticles. International Polymer Science and Technology. 2010; 37:T59-T64.
5. Azlin-Hasim S, Cruz-Romero MC, Ghoshal T, Morris MA, Cummins E, Kerry JP, et al. Application of silver nanodots for potential use in antimicrobial packaging applications. Innovative Food Science & Emerging Technologies. 2015; 27:136-143.
6. Azlin-Hasim S, Cruz-Romero MC, Cummins E, Kerry JP, Morris MA. The potential use of a layer-by-layer strategy to develop LDPE antimicrobial films coated with silver nanoparticles for packaging applications. Journal of Colloid and Interface Science. 2016; 461:239-248.
7. Azlin-Hasim S. The Potential Application of Antimicrobial Silver Polyvinyl Chloride Nanocomposite Films to Extend the Shelf-Life of Chicken Breast Fillets. Food and Bioprocess Technology. 2016; 9:1661-1673.
8. Hannon JC, Kerry JP, Cruz-Romero MC, Azlin-Hasim S, Morris M, Cummins E. Kinetic desorption models for the release of nanosilver from an experimental nanosilver coating on polystyrene food packaging. Innovative Food Science & Emerging Technologies. 2017.
9. Appendini P, Hotchkiss JH. Review of antimicrobial food packaging. Innovative Food Science & Emerging Technologies. 2002; 3:113-126.
10. AshaRani PV, Kah Mun GL, Hande MP, Valiyaveettil S. Cytotoxicity and Genotoxicity of Silver Nanoparticles in Human Cells. ACS Nano. 2009; 3:279-290.
11. Nel A, Xia T, Mädler L, Li N. Toxic Potential of Materials at the Nanolevel. Science. 2006; 311:622-627.
12. Takenaka S, Karg E, Roth C, Schulz H, Ziesenis A, Heinzmann U, et al. Pulmonary and systemic distribution of inhaled ultrafine silver particles in rats. Environmental Health Perspectives. 2001; 109(Suppl 4):547-551.
13. Tomankova K, Horakova J, Harvanova M, Malina L, Soukupova J, Hradilova S, et al. et al., Cytotoxicity, cell uptake and microscopic analysis of titanium dioxide and silver nanoparticles in vitro. Food Chem Toxicol. 2015; 82:106-15.
14. Li Y, Zhang W, Niu J, Chen Y. Surface-Coating-Dependent Dissolution, Aggregation, and Reactive Oxygen Species (ROS) Generation of Silver Nanoparticles under Different Irradiation Conditions. Environmental Science & Technology. 2013; 47:10293-10301.
15. Carlson C, Hussain SM, Schrand AM, Braydich-Stolle LK, Hess KL, Jones RL, et al., Unique cellular interaction of silver nanoparticles: size-dependent generation of reactive oxygen species. J Phys Chem B. 2008; 112:13608-19.
16. El Badawy AM, Silva RG, Morris B, Scheckel KG, Suidan MT, Tolaymat TM. Surface Charge-Dependent Toxicity of Silver Nanoparticles. Environmental Science & Technology. 2011; 45:283-287.
17. Choi O, Hu. Size dependent and reactive oxygen species related nanosilver toxicity to nitrifying bacteria. Environ Sci Technol. 2008; 42:4583-8.
18. Liu J, Sonshine DA, Shervani S, Hurt RH. Controlled Release of Biologically Active Silver from Nanosilver Surfaces. ACS Nano. 2010; 4:6903-6913.
19. Liu W, Wu Y, Wang C, Li HC, Wang T, Liao CY, et al. Impact of silver nanoparticles on human cells: effect of particle size. Nanotoxicology. 2010; 4:319-30.
20. Suresh AK, Pelletier DA, Wang W, Morrell-Falvey JL, Gu B, Doktycz MJ. Cytotoxicity induced by engineered silver nanocrystallites is dependent on surface coatings and cell types. Langmuir. 2012; 28:2727-35.
21. Sondi I, Salopek-Sondi B. Silver nanoparticles as antimicrobial agent: a case study on E. coli as a model for Gram-negative bacteria. J Colloid Interface Sci. 2004; 275.
22. Christopher, Linic S. Shape- and Size-Specific Chemistry of Ag Nanostructures in Catalytic Ethylene Epoxidation. ChemCatChem. 2010; 2:78-83.
23. Ioan-Avram N, Ficai A, Sonmez M, Ficai D, Oprea O, Andronesu E. Silver Based Materials for Biomedical Applications. Current Organic Chemistry. 2014; 18:173-184.
24. Bruni S, Guglielmi V, Pozzi F. Surface-enhanced Raman spectroscopy (SERS) on silver colloids for the identification of ancient textile dyes: Tyrian purple and madder. Journal of Raman Spectroscopy. 2010; 41:175-180.
25. Choi O, Hu Z. Size Dependent and Reactive Oxygen Species Related Nanosilver Toxicity to Nitrifying Bacteria. Environmental Science & Technology. 2008; 42:4583-4588.
26. Gliga AR, Skoglund S, Wallinder IO, Fadeel B, Karlsson HL. Size-dependent cytotoxicity of silver nanoparticles in human lung cells: the role of cellular uptake, agglomeration and Ag release. Part Fibre Toxicol. 2014; 11:11.
27. Rivera-Gil P, Jimenez de Aberasturi D, Wulf V, Pelaz B, del Pino P, Zhao Y, et al. The Challenge To Relate the Physicochemical Properties of Colloidal Nanoparticles to Their Cytotoxicity. Accounts of Chemical Research. 2013; 46:743-749.
28. Aherne D, Ledwith DM, Gara M, Kelly JM. Optical Properties and Growth Aspects of Silver Nanoprisms Produced by a Highly Reproducible and Rapid Synthesis at Room Temperature. Advanced Functional Materials. 2008; 18:2005-2016.
29. Singh RP, Ramarao P, Cellular uptake, intracellular trafficking and cytotoxicity of silver nanoparticles. Toxicol Lett. 2012; 213:249-59.
30. Shang L, Nienhaus K, Nienhaus GU. Engineered nanoparticles interacting with cells: size matters. J Nanobiotechnology. 2014; 12:5.
31. Böhme S, Stärk HJ, Meißner T, Springer A, Reemtsma T, Kühnel D, et al. Quantification of Al2O3 nanoparticles in human cell lines applying inductively coupled plasma mass spectrometry (neb-ICP-MS, LA-ICP-MS) and flow cytometry-based methods. J Nanopart Res. 2014; 16:2592.
32. Liu J, Hurt RH. Ion Release Kinetics and Particle Persistence in Aqueous Nano-Silver Colloids. Environmental Science & Technology. 2010; 44:2169-2175.
33. Zanette C, Pelin M, Crosera M, Adami G, Bovenzi M, Larese FF, et al. Silver nanoparticles exert a long-lasting antiproliferative effect on human keratinocyte HaCaT cell line. Toxicology in Vitro. 2011; 25:1053-1060.
34. Gengan RM, Anand K, Phulukdaree A, Chuturgoon A. A549 lung cell line activity of biosynthesized silver nanoparticles using Albizia adianthifolia leaf. Colloids Surf B Biointerfaces. 2013; 105:87-91.
35. Ong KJ, MacCormack TJ, Clark RJ, Ede JD, Ortega VA, Felix LC, et al. Widespread Nanoparticle-Assay Interference: Implications for Nanotoxicity Testing. PLOS ONE. 2014; 9:e90650.
36. Oh SJ, Kim H, Liu Y, Han HK, Kwon K, Chang KH, et al., Incompatibility of silver nanoparticles with lactate dehydrogenase leakage assay for cellular viability test is attributed to protein binding and reactive oxygen species generation. Toxicol Lett. 2014; 225:422-32.
37. Morris MA, Padmanabhan SC, Cruz-Romero MC, Cummins E, Kerry JP. Development of active, nanoparticle, antimicrobial technologies for muscle-based packaging applications. Meat Science. 2017; 132(Supplement C):163-178.